

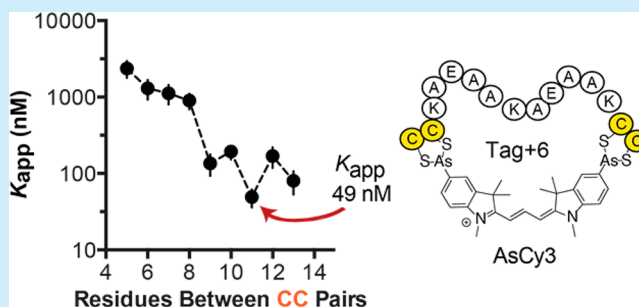
## Interactions of AsCy3 with Cysteine-Rich Peptides

Seth C. Alexander<sup>†</sup> and Alanna Schepartz<sup>\*,†,‡</sup>

<sup>†</sup>Department of Chemistry and <sup>‡</sup>Department of Molecular, Cellular and Developmental Biology, Yale University, New Haven, Connecticut 06520-8107, United States

**S** Supporting Information

**ABSTRACT:** There is great interest in fluorogenic compounds that tag biomolecules within cells. Biarsenicals are fluorogenic compounds that become fluorescent upon binding four proximal Cys thiols, a tetracysteine (Cys<sub>4</sub>) motif. This work details interactions between the biarsenical AsCy3 and Cys<sub>4</sub> peptides. Maximal affinity was observed when two Cys-Cys pairs were separated by at least 8 amino acids; the highest affinity ligand bound in the nanomolar concentration range ( $K_{app} = 43$  nM) and with a significant (3.2-fold) fluorescence enhancement.



There is great interest in the identification of fluorogenic compounds that tag biomolecules within cells. Molecules with these properties, especially those that are bright, specific, and nontoxic, can often extract high-resolution information from within a complex, heterogeneous environment.<sup>1</sup> When the biomolecule is a protein, fluorogenic compounds can define intracellular location, monitor protein–protein interactions, discriminate conformations, and quantify protein activity. Biarsenical dyes,<sup>2</sup> exemplified by FAsH<sup>3</sup> and ReAsH,<sup>4</sup> represent one such class of fluorogenic compound. These compounds are distinguished by a fluorescence enhancement that occurs upon binding to proteins containing four proximal Cys thiols, a tetracysteine (Cys<sub>4</sub>) motif. Over the past dozen years, fluorogenic biarsenicals have been used to label and visualize  $\beta$ -tubulin,<sup>5</sup> monitor amyloid formation,<sup>6</sup> localize viruses,<sup>7</sup> probe transmembrane  $\alpha$ -helix interactions and orientations,<sup>8</sup> and evaluate conformational changes in the  $\beta_2$ -<sup>9</sup> and  $\alpha_{2A}$ -adrenergic receptors,<sup>10</sup> among other applications.<sup>11</sup>

These important discoveries notwithstanding, the application of FAsH and ReAsH to discover new biology (especially within the cell) is limited by strong background labeling and relatively weak fluorescence.<sup>2,4</sup> Background labeling results from the interaction of FAsH and ReAsH with nonspecific thiols as well as membranes and hydrophobic protein pockets.<sup>2</sup> Even with an improved binding sequence,<sup>12</sup> ReAsH is still less bright than common fluorophores such as Alexafluor-488 and BODIPY FL. Moreover, despite the differences in their emission maxima (528 and 608 nm, respectively) the similarity of the FAsH and ReAsH structures prohibits their use in simultaneous two-color labeling experiments.<sup>4</sup>

Recently we applied the biarsenical ReAsH in a bipartite mode<sup>13</sup> along with total internal reflectance microscopy (TIR-FM) to detect, characterize, and differentiate ligand-induced conformational changes within the epidermal growth factor receptor (EGFR) on the mammalian cell surface.<sup>13,14</sup> Through the design of EGFR variants with Cys-Cys pairs within the

cytosolic juxtamembrane (JM) segment, we discovered that the binding of the growth factor EGF induced the formation of an anti-parallel coiled coil within the JM that was functionally linked to kinase activation. Other growth factors, most notably TGF- $\alpha$ , induced a different structure.<sup>13,14</sup> Our ability to probe and differentiate structures within the juxtamembrane segment would be greatly enhanced by an alternative to FAsH and ReAsH, especially one that was bright and photostable and could detect and report on alternative Cys<sub>4</sub> motifs.

One molecule with some potential in this regard, AsCy3 (Figure 1A), was reported in 2007.<sup>15</sup> In AsCy3 the biarsenical motif is displayed on a Cy3 scaffold and was reported to bind the alternative Cys<sub>4</sub> motif Cys-Cys-Lys-Ala-Glu-Ala-Ala-Cys-Cys with a brightness comparable to that of ReAsH ( $5.0 \times 10^4$  M<sup>-1</sup> cm<sup>-1</sup>)<sup>4,10</sup> and significantly greater (>30-fold) photostability.<sup>15</sup> Since 2007, AsCy3 has been transformed into a super-resolution probe<sup>16</sup> and a membrane-permeable dye via substitution of the anionic sulfonate side chains for methyl esters,<sup>17</sup> and the monoarsenic variant has explored dithiol oxidation in bacteria.<sup>18</sup> Here we report that the initially described Cys<sub>4</sub> motif binds AsCy3 with only modest affinity and fluorescent enhancement, but that higher affinity (100-fold) and brightness (>3-fold) is seen with the expanded Cys<sub>4</sub> motif Cys-Cys-Lys-Ala-Glu-Ala-Ala-Lys-Ala-Glu-Ala-Ala-Lys-Cys-Cys. We hope that this information will aid researchers as they apply AsCy3 to characterize protein interactions on the cell surface and ultimately within the cytosol.

AsCy3 was synthesized following a modified procedure (Scheme S1 in Supporting Information), and its identity was confirmed with <sup>1</sup>H and <sup>13</sup>C NMR and high-resolution mass spectrometry. When dissolved at 10  $\mu$ M in 50 mM HEPES (pH 7.5) containing 10% DMSO, the parent Cy3 displayed an absorbance maximum at 546 nm ( $\epsilon_{546} = 126,000$  M<sup>-1</sup> cm<sup>-1</sup>)

Received: June 17, 2014

Published: July 7, 2014

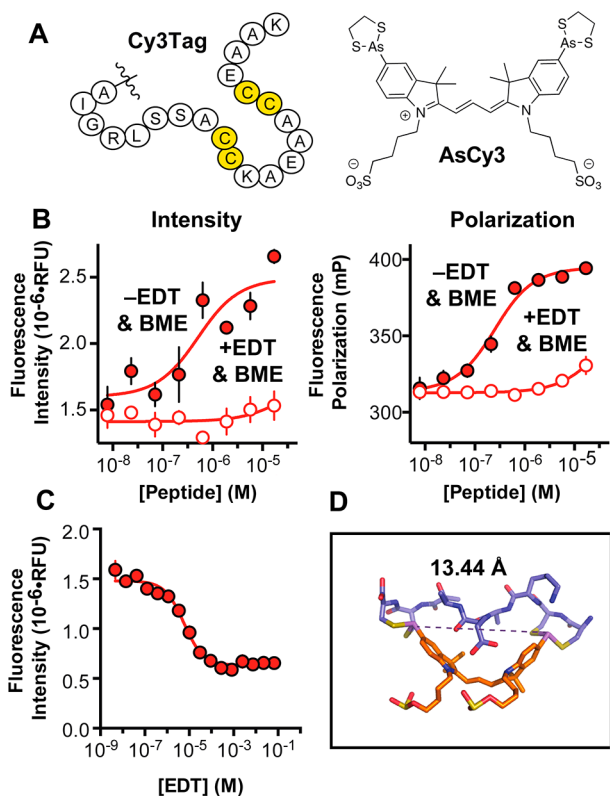


**Figure 1.** AsCy3 and its interactions with Cy3Tag. (A) Sequence of Cy3Tag (left) and structure of AsCy3 (right). (B) Plots illustrating the changes in FI (left) and FP (right) of 0.1  $\mu\text{M}$  AsCy3 after incubation with the [Cy3Tag] indicated in the presence (closed) and absence (open) of 100  $\mu\text{M}$  EDT and 1 mM BME. (C) Competition between 10  $\mu\text{M}$  Cy3Tag and [EDT] for 0.1  $\mu\text{M}$  AsCy3, measured by changes in FI. Errors show standard error. (D) Minimized structure (Gaussian) of the hypothetical complex between AsCy3 and Cy3Tag.

and a emission maximum at 557 nm (Figure S1 in Supporting Information). These values compare well with those in methanol, where an absorbance maximum at 549 nm ( $\epsilon_{549} = 120,000 \text{ M}^{-1} \text{ cm}^{-1}$ ) was reported.<sup>19</sup> Both the absorbance and emission maxima of AsCy3 are red-shifted relative to Cy3; under identical conditions AsCy3 exhibited maximal absorbance at 564 nm ( $\epsilon_{564} = 103,000 \text{ M}^{-1} \text{ cm}^{-1}$ ) and maximal emission at 575 nm (Figure S1 in Supporting Information). These values differ slightly from those reported:  $\lambda_{\text{max}} = 560 \text{ nm}$  (absorbance,  $\epsilon_{560} = 180,000 \text{ M}^{-1} \text{ cm}^{-1}$ );  $\lambda_{\text{max}} = 568 \text{ nm}$  (emission).

The initial AsCy3 report described interactions with Cy3Tag, a 34-aa peptide containing two Cys-Cys motifs separated by the sequence Lys-Ala-Glu-Ala-Ala (Figure 1A). As reported, the complex formed with an equilibrium dissociation constant ( $K_{\text{app}}$ ) of  $80 \pm 10 \text{ nM}$ , calculated on the basis of Cy3Tag-dependent changes in fluorescence intensity at 576 nm. We repeated the titration of AsCy3 with Cy3Tag, monitoring changes in both fluorescence polarization (FP, which measures binding directly) and fluorescence intensity (FI, which does not). Experiments were performed initially under the conditions reported: HEPES buffer containing 10% DMSO, 140 mM KCl, 1 mM TCEP, 100  $\mu\text{M}$  EDT, and 1 mM BME. No interaction between AsCy3 and Cy3Tag was observed under these conditions whether the association was monitored by changes in FI or FP at Cy3Tag concentrations as high as 15  $\mu\text{M}$  (Figure 1B). However, in a buffer lacking the competitive

inhibitors EDT and BME, concentration-dependent changes in both FP and FI were observed. In each case, the data fit a simple 1:1 equilibrium-binding isotherm to provide  $K_{\text{app}}$  values of  $970 \pm 140 \text{ nM}$  (FI) and  $2.4 \pm 0.6 \mu\text{M}$  (FP). These values are at least an order of magnitude higher than those reported by Cao et al.<sup>15</sup> and were obtained only in the absence of thiol competitors. Competition of the AsCy3-Cy3Tag complex with EDT yielded an inhibition constant ( $K_i$ ) of  $5.6 \pm 0.9 \mu\text{M}$ , a value only slightly higher than the  $K_{\text{app}}$  values determined for the Cy3Tag complex, providing additional evidence for a low-affinity AsCy3-Cy3Tag interaction. Although cyanine dyes such as AsCy3 can aggregate,<sup>20</sup> our experimental setup minimizes the effect of [AsCy3] on the calculated  $K_{\text{app}}$  (see Supporting Information).

The interactions between AsCy3 and Cy3Tag were also studied by characterizing the changes in the fluorescence spectrum of AsCy3 in the presence of Cy3Tag (Figure S1C in Supporting Information). Upon incubation of 100 nM AsCy3 (in 50 mM HEPES pH 7.5, 140 mM KCl, and 1 mM TCEP) with 10  $\mu\text{M}$  Cy3Tag, the emission maximum was maintained at 575 nm as expected,<sup>15</sup> but fluorescence emission was increased by only 2.5-fold, significantly less than the reported 6-fold increase under similar conditions.<sup>15</sup>

These results prompted us to evaluate the structure of AsCy3 and its complex with Cy3Tag. The ground state geometry of AsCy3 bound to two ethanedithiol (EDT) ligands (calculated using Gaussian 09<sup>21</sup> and the internal molecular mechanics UFF package) was characterized by an interatomic As-As distance of 15.83 Å, a value longer than that between the  $\alpha$ -carbons of residues  $i$  and  $i + 7$  on a canonical  $\alpha$ -helix (10.8 Å), the proposed target site for AsCy3.<sup>15</sup> Calculation of the ground state geometry of AsCy3 bound to Cys-Cys-Lys-Ala-Glu-Ala-Ala-Cys-Cys suggested a compressed interatomic As-As distance (13.44 Å) and a non- $\alpha$ -helical peptide backbone (Figure 1D). Furthermore, in the calculated complex, AsCy3 was nonplanar, with a  $> 100^\circ$  angle between the normal vectors to the two indole ring planes (Figure S2 in Supporting Information). Cy3 fluorophores demand a planar, conjugated  $\pi$  system to achieve significant quantum yields.<sup>22</sup> These calculations imply a mismatch between the structure of AsCy3 and the most favorable disposition(s) of Cys-Cys ligands on Cy3Tag. They also suggest two factors that could contribute to the low AsCy3-Cy3Tag affinity: (1) interaction of AsCy3 with only one Cys-Cys motif (not two) and (2) strain energy associated with forming the Cys4-coordinate complex. More importantly, the calculations suggest that target sites with longer intervening sequences would better match the AsCy3 structure and permit the formation of a more planar, higher-affinity, and more fluorogenic complex.

To better explore the AsCy3-Cy3Tag binding mode, we synthesized a pair of Cy3Tag variants in which one (Tag $\Delta$ 2) or both (Tag $\Delta$ 4) Cys-Cys motifs were replaced by Ala-Ala (Figure 2A). The interactions of Tag $\Delta$ 2 and Tag $\Delta$ 4 with AsCy3 were evaluated by monitoring changes in both fluorescence intensity (Figure 2B) and fluorescence polarization (Figure 2C) as a function of peptide concentration. Only Tag $\Delta$ 2 showed evidence of an interaction with AsCy3 (Figure 2B). As was true for the Cy3Tag interaction, the data could be fit to a 1:1 binding isotherm, yielding a  $K_{\text{app}}$  value of  $960 \pm 150 \text{ nM}$  based on fluorescence intensity changes and  $K_{\text{app}} = 410 \pm 92 \text{ nM}$  based on changes in fluorescence polarization. These  $K_{\text{app}}$  values equal or exceed those determined for Cy3Tag itself, depending on the method (FI,  $970 \pm 140 \text{ nM}$ ; FP,  $2.3 \pm 0.6$

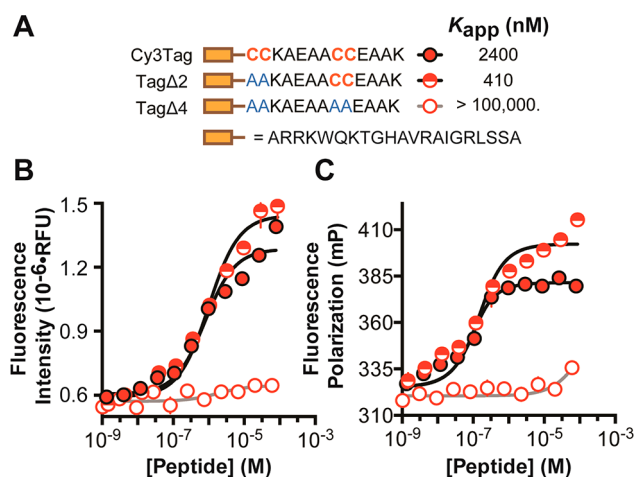


**Figure 2.** Interactions of AsCy3 with Cy3Tag and variants. (A) Sequence of Cy3Tag, Tag $\Delta$ 2, and Tag $\Delta$ 4 with  $K_{app}$  values determined by FP. (B) Plot of the FI of 100 nM AsCy3 after incubation with the Cy3Tag, Tag $\Delta$ 2, and Tag $\Delta$ 4. (C) Plot of the FP under identical conditions. Error bars show standard error.

$\mu$ M). The observation that AsCy3 interacts comparably with peptides containing one or two Cys-Cys motifs suggests that only one Cys-Cys pair in the Cy3Tag sequence contributes to complex stability.<sup>18</sup> Indeed, the change in AsCy3 fluorescence emission (100 nM) in the presence of Tag $\Delta$ 2 (10  $\mu$ M) is >60% of the enhancement observed with CyTag. This observation indicates that the second Cys-Cys pair contributes minimally, if at all, to AsCy3 fluorogenicity, and the dye may only be partially bound to all four cysteines (Figure S1C in Supporting Information).

Next, we synthesized a second set of potential AsCy3 ligands containing progressively longer intervening sequences and evaluated their interactions with AsCy3 using fluorescence intensity and polarization assays (Figure 3). These potential

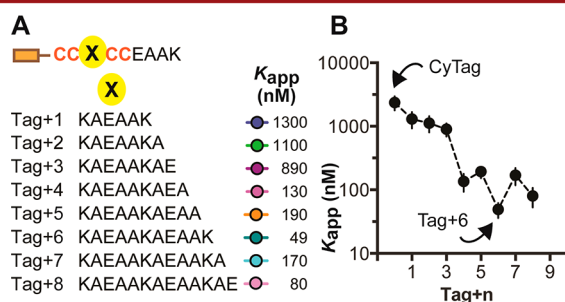


**Figure 3.** Interactions of AsCy3 with Tag+n sequences. (A) Sequences of potential AsCy3 ligands and  $K_{app}$  values determined by FP. (B) Plot illustrating relationship between  $K_{app}$  and the number of amino acids separating the Cys-Cys motifs ( $n$ ).

AsCy3 ligands contained from 6 to 13 amino acids interposed between the two Cys-Cys motifs and were largely unstructured at 30  $\mu$ M in the absence of AsCy3, as judged by circular dichroism (CD) spectroscopy (5 mM phosphate (pH 7.5), 140 mM KCl, and 5 mM DTT) (Figure S3 in Supporting Information). All of the second-generation peptides evaluated formed complexes with AsCy3, exhibiting  $K_{app}$  values between 49 nM and 1.3  $\mu$ M in the absence of EDT and BME. With one exception (Tag+2), the values determined using FI and FP agreed to within their 95% confidence intervals (Table S1 in

Supporting Information). Notably, the fitted value of  $K_{app}$  decreased as the number of residues between the two Cys-Cys motifs increased from 5 to 9, with the largest increase between Tag+3 and Tag+4 (Figure S4 in Supporting Information). The highest affinity ligand was Tag+6, whose AsCy3 complex was characterized by a  $K_{app}$  value of  $94 \pm 16$  nM (FI);  $K_{app} = 49 \pm 13$  nM by fluorescence polarization. Titration of AsCy3 (100 nM) and Tag+6 (30  $\mu$ M) with between 5 nM and 10  $\mu$ M EDT led to a systematic decrease in fluorescence emission at 580 nm. This decrease could be fit to yield an inhibition constant ( $K_i$ ) of  $9.3 \pm 4.6$   $\mu$ M (Figure S5 in Supporting Information), in agreement with the value determined on the basis of competition with CyTag ( $K_i = 5.6 \pm 0.9$   $\mu$ M). Thus, Tag+6 binds AsCy3 more than 100 times more favorably than EDT or CyTag.

A final set of experiments was performed to provide additional resolution of the binding mode. Substitution of one Cys-Cys motif within Tag+6 to generate Tag+6 $\Delta$ 2 led to a 50-fold loss in equilibrium binding affinity, in contrast to the minimal changes observed upon removal of a single Cys-Cys motif from CyTag. The Tag+6 $\Delta$ 2-AsCy3 complex is characterized by a  $K_{app}$  value of  $1.4 \pm 0.36$   $\mu$ M by FP (FI,  $860 \pm 160$  nM) (Figure 4), values very similar to those of

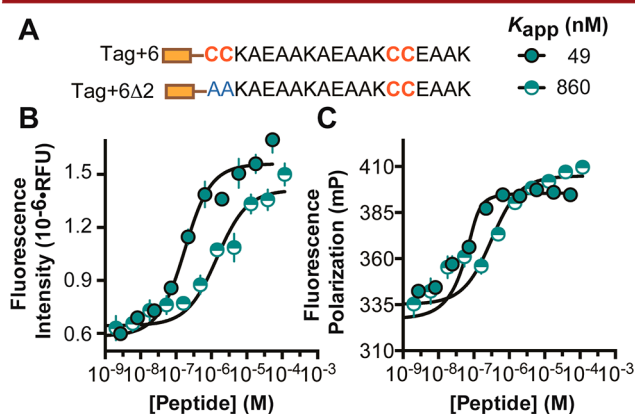


**Figure 4.** Interactions of AsCy3 with Tag+6 and Tag+6 $\Delta$ 2. (A) Sequences of Tag+6 and Tag+6 $\Delta$ 2 with  $K_{app}$  values measured by FP. (B) Plot of the FI of 100 nM AsCy3 after incubation with the indicated [Tag+6] and [Tag+6 $\Delta$ 2]. (C) Plot of the FP under identical conditions. Error bars represent the standard error.

Cy3Tag itself, providing additional evidence that the Cy3Tag interacts minimally with the second Cys-Cys motif in CyTag. Incubation of Tag+6 with AsCy3 led to an overall 3.2-fold increase in fluorescence, compared to only a 1.5-fold increase in the case of Tag+6 $\Delta$ 2 (Figure S1C in Supporting Information).

In summary, we describe a detailed characterization of the interactions between AsCy3<sup>15</sup> and various cysteine-rich peptides. Maximal affinity was observed with Cys<sub>4</sub> sequences in which the two Cys-Cys pairs were separated by at least 8 amino acids; the highest affinity ligand was Tag+6, whose complex with AsCy3 assembled in the nanomolar concentration range ( $K_{app} = 43$  nM) and was characterized by a significant (3.2-fold) fluorescence enhancement. We hope that this information will aid other researchers as they apply AsCy3 to characterize protein interactions on the cell surface or ultimately within the cytosol.

**■ ASSOCIATED CONTENT****■ Supporting Information**

Experimental procedures and data. This material is available free of charge via the Internet at <http://pubs.acs.org>.

**■ AUTHOR INFORMATION****Corresponding Author**

\*E-mail: [Alanna.schepartz@yale.edu](mailto:Alanna.schepartz@yale.edu).

**Notes**

The authors declare no competing financial interest.

**■ ACKNOWLEDGMENTS**

We gratefully acknowledge the NIH for support of this work (GM 83257).

**■ REFERENCES**

- (1) Lowder, M. A.; Appelbaum, J. S.; Hobert, E. M.; Schepartz, A. *Curr. Opin. Chem. Biol.* **2011**, *15*, 781.
- (2) Scheck, R. A.; Schepartz, A. *Acc. Chem. Res.* **2011**, *44*, 654.
- (3) Griffin, B. A.; Adams, S. R.; Tsien, R. Y. *Science* **1998**, *281*, 269.
- (4) Adams, S. R.; Campbell, R. E.; Gross, L. A.; Martin, B. R.; Walkup, G. K.; Yao, Y.; Llopis, J.; Tsien, R. Y. *J. Am. Chem. Soc.* **2002**, *124*, 6063.
- (5) Andresen, M.; Schmitz-Salue, R.; Jakobs, S. *Mol. Biol. Cell* **2004**, *15*, 5616.
- (6) Roberti, M. J.; Bertocini, C. W.; Klement, R.; Jares-Erijman, E. A.; Jovin, T. M. *Nat. Methods* **2007**, *4*, 345.
- (7) (a) Rudner, L.; Nydegger, S.; Coren, L. V.; Nagashima, K.; Thali, M.; Ott, D. E. *J. Virol.* **2005**, *79*, 4055. (b) Panchal, R. G.; Ruthel, G.; Kenny, T. A.; Kallstrom, G. H.; Lane, D.; Badie, S. S.; Li, L.; Bavari, S.; Aman, M. J. *Proc. Natl. Acad. Sci. U.S.A.* **2003**, *100*, 15936. (c) Wu, L.; Huang, T.; Yang, L.; Pan, J.; Zhu, S.; Yan, X. *Angew. Chem., Int. Ed.* **2011**, *50*, 5873.
- (8) Pace, C. J.; Huang, Q.; Wang, F.; Palla, K. S.; Fuller, A. A.; Gao, J. *Chem. Biochem.* **2011**, *12*, 1018.
- (9) Nakanishi, J.; Takarada, T.; Yunoki, S.; Kikuchi, Y.; Maeda, M. *Biochem. Biophys. Res. Commun.* **2006**, *343*, 1191.
- (10) Hoffmann, C.; Gaietta, G.; Bünemann, M.; Adams, S. R.; Oberdorff-Maass, S.; Behr, B.; Vilardaga, J. P.; Tsien, R. Y.; Ellisman, M. H.; Lohse, M. J. *Nat. Methods* **2005**, *2*, 171.
- (11) (a) Dyachok, O.; Isakov, Y.; Sâgetorp, J.; Tengholm, A. *Nature* **2006**, *439*, 349. (b) Enninga, J.; Mounier, J.; Sansonetti, P.; Nhieu, G. T. V. *Nat. Methods* **2005**, *2*, 959. (c) Fujii, T.; Shindo, Y.; Hotta, K.; Citterio, D.; Nishiyama, S.; Suzuki, K.; Oka, K. *J. Am. Chem. Soc.* **2014**, *136*, 2374. (d) Wlodarchak, N.; Guo, F.; Satyshur, K. A.; Jiang, L.; Jeffrey, P. D.; Sun, T.; Stanevich, V.; Mumby, M. C.; Xing, Y. *Cell Res.* **2013**, *23*, 931. (e) Tsytlonok, M.; Itzhaki, L. S. *Chem. Biochem.* **2012**, *13*, 1199. (f) Poëa-Guyon, S.; Ammar, M. R.; Erard, M.; Amar, M.; Moreau, A. W.; Fossier, P.; Gleize, V.; Vitale, N.; Morel, N. *J. Cell Biol.* **2013**, *203*, 283. (g) Irtegun, S.; Wood, R.; Lackovic, K.; Schweiggert, J.; Ramdzan, Y. M.; Huang, D. C. S.; Mulhern, T. D.; Hatters, D. M. *ACS Chem. Biol.* **2014**, DOI: 10.1021/cb500242q.
- (12) Martin, B. R.; Giepmans, B. N. G.; Adams, S. R.; Tsien, R. Y. *Nat. Biotechnol.* **2005**, *23*, 1308.
- (13) (a) Goodman, J. L.; Fried, D. B.; Schepartz, A. *Chem. Biochem.* **2009**, *10*, 1644. (b) Luedtke, N. W.; Dexter, R. J.; Fried, D. B.; Schepartz, A. *Nat. Chem. Biol.* **2007**, *3*, 779.
- (14) Scheck, R. A.; Lowder, M. A.; Appelbaum, J. S.; Schepartz, A. *ACS Chem. Biol.* **2012**, *7*, 1367.
- (15) Cao, H.; Xiong, Y.; Wang, T.; Chen, B.; Squier, T. C.; Mayer, M. U. *J. Am. Chem. Soc.* **2007**, *129*, 8672.
- (16) Fu, N.; Xiong, Y.; Squier, T. C. *J. Am. Chem. Soc.* **2012**, *134*, 18530.
- (17) Fu, N.; Xiong, Y.; Squier, T. C. *Bioconjugate Chem.* **2013**, *24*, 251.

(18) Fu, N.; Su, D.; Cort, J. R.; Chen, B.; Xiong, Y.; Qian, W.-J.; Konopka, A. E.; Bigelow, D. J.; Squier, T. C. *J. Am. Chem. Soc.* **2013**, *135*, 3567.

(19) Peng, Z.-H.; Qun, L.; Zhou, X.-F.; Carroll, S.; Geise, H. J.; Peng, B.-X.; Dommissie, R.; Carleer, R. *J. Mater. Chem.* **1996**, *6*, 559.

(20) Mishra, A.; Behera, R. K.; Behera, P. K.; Mishra, B. K.; Behera, G. B. *Chem. Rev.* **2000**, *100*, 1973.

(21) Frisch, M. J.; Trucks, G. W.; Schlegel, H. B.; Scuseria, G. E.; Robb, M. A.; Cheeseman, J. R.; Scalmani, G.; Barone, V.; Mennucci, B.; Petersson, G. A.; Nakatsuji, H.; Caricato, M.; Li, X.; Hratchian, H. P.; Izmaylov, A. F.; Bloino, J.; Zheng, G.; Sonnenberg, J. L.; Hada, M.; Ehara, M.; Toyota, K.; Fukuda, R.; Hasegawa, J.; Ishida, M.; Nakajima, T.; Honda, Y.; Kitao, O.; Nakai, H.; Vreven, T.; Montgomery, J. A., Jr.; Peralta, J. E.; Ogliaro, F.; Bearpark, M.; Heyd, J. J.; Brothers, E.; Kudin, K. N.; Staroverov, V. N.; Kobayashi, R.; Normand, J.; Raghavachari, K.; Rendell, A.; Burant, J. C.; Iyengar, S. S.; Tomasi, J.; Cossi, M.; Rega, N.; Millam, J. M.; Klene, M.; Knox, J. E.; Cross, J. B.; Bakken, V.; Adamo, C.; Jaramillo, J.; Gomperts, R.; Stratmann, R. E.; Yazyev, O.; Austin, A. J.; Cammi, R.; Pomelli, C.; Ochterski, J. W.; Martin, R. L.; Morokuma, K.; Zakrzewski, V. G.; Voth, G. A.; Salvador, P.; Dannenberg, J. J.; Dapprich, S.; Daniels, A. D.; Farkas, Ö.; Foresman, J. B.; Ortiz, J. V.; Cioslowski, J.; Fox, D. J. *Gaussian 09, Revision D.01*; Gaussian, Inc.: Wallingford, CT, 2009.

(22) Randolph, J. B.; Waggoner, A. D. *Nucl. Acids Res.* **1997**, *25*, 2923–2929. Karaca, S.; Elmaci, N. *Comp. Theor. Chem.* **2011**, *964*, 160–168.